Advanced Structural Fibre Material for Single Link Robotic Manipulator Simulation Analysis with Flexibility

Submitted: 7th March 2019; accepted: 20th December 2019

S. Ramalingam, S. Rasool Mohideen

DOI: 10.14313/JAMRIS/4-2019/36

Abstract: *The aim of this article is to investigate the characteristics of a composite fibre advanced materials used as a robotic link manipulator for replacement of rigid one. The composite material is combination of two and more fibre processed and bonded with epoxy, resulting hybrid form of material component with required properties which are to be analyzed for suitability with respect to its function, reliability, durability, safety and cost-effectiveness. The composites generally have high-strength, high-stiffness (graphite, kevlar, etc.) low-density (epoxy, polyvinyl) strong and stiff with lightweight. In this investigation, five different composite structural fibres are taken as a flexible link with joint flexibility for case study analysis. The rotating structural fibre link, loaded and tested different types of joint stiffness coefficients (k_c). The numerical evaluations are conducted for structural fibre material for replacement rigid manipulator. The modeling of structural fibre single flexible link on the basis of Euler-Bernoulli beam theory and Lagrange's equations of motion is studied and accurate modes of the system are obtained.*

Keywords: *Structural fibre, E – Glass, S – Glass, Kevlar-29, Carbon fibres, Dynamic Model, Simulation, Vibration*

1. Introduction

The flexible link materials in a robotic system are capable of changing their structural configuration while being able to maneuver through highly cluttered and constrained environments. The mechanical flexibilities on the manipulator can be added in both the links and joints of the manipulator. Link flexibility reduces the weight of the link that is designed to operate at high speed with low inertia [1]. The soft-link manipulators have certain merits like, low costs, easy industrial fabrication process. The flexible link has a lower stiffness than metal; the soft link material manipulator can reduce the damage from impact loads, when the robot is used to handle material from one place to another, material storage controlling of material and protection of materials [2]. The conventional material robotic link systems generally made of rigid type, such as steel and aluminum and are dominated in many successful applications [3]. A robotic link that fulfills the requirements like work assignment, safety, reliability, durability and cost-effectiveness are considered in design of manipulator. In the other applications like land transport system, Marine vessels for inland and water ways, ocean structures such as boats, ships, pontoons, harbor structures, buoys, underwater structures, submarines composite material is used, and the other areas such as aerospace, defense, security systems, energy appliances, Thermal, hydroelectric, wind, solar, wave energy etc. the flexible material is used. Robotic manipulators are also used, including manufacturing industrial automation, power plant stations, materials fabrication and space stations maintenance and surgery in the clinical field [4].

However, the studies of flexible robots, which generally make use of an elastic and flexible type material, are now drawing more attention in research area [5]. The flexible soft robots have additional properties relative to conventional rigid robot manipulators [6-8]. These hard and rigid robots are usually performing limited actions with high precision with the help of sensors and feedback control system in well-defined environments. But flexible robots have distributed deformation with infinite number of degrees of freedom and also capable entering into an obstacle place. This leads to an idea of introducing new type of material for robotic manipulator. Due to technology update, ranging from new materials and process techniques, to new design and control tools, it is now becoming possible to create systems whose structure is composed almost entirely of flexible structural materials. These systems are composites of flexible materials that together give rise to entirely new modes of function and behavior, in many ways [9].

Introducing lightweight manipulators have plenty of advantages such as reduced inertia, minimize the gravity effect on link and drives have been discussed in this article. The joint flexibility increases whole structure flexibility, which helps to derive accurate dynamic model for control purpose and perform a critical task carried by the robot end link via obstacle point to the exact location. The next generation of light weight robots like humanoid robots, soft robots, micro surgery and composite artificial links will also introduce flexible joints. The flexible joint has an elastic property and serves as an energy storage device; it helps the system in terms of the energy consumption for the same motion of the link. Future generation of lightweight robots with variable joint stiffness of humanoids robots will implement flexible joints are active research. Hence light weight manipulators with flexible joint in robotic system have prime importance issue in dynamic modeling and simulation analysis. The importance of mechanical flexibility, how it is critical in design and fabrication of flexible robot in initial stage are briefed. For this purpose, composite materials fibre are taken as link material for simulation and numerical study. The mode of vibration is the characteristic patterns assumed by the system are to be drawn with shape of maximum displacement curve due to vibration. The mode shapes are plotted and analyzed for control system purpose.

2. Material and Methods

2.1. Composite Fibre Materials

The hybrid composites are a kind of fibre-reinforced materials; it is usually resin-based, in which two different fibres are integrated into a single matrix [10]. The simple theory of composite is of combining two or more materials to get the required properties of materials. In any combination of dissimilar materials could in fact be thought of as a hybrid. The example for structural material is rigid plastic foam bonded with thin skins of some high-performance FRPs. The skin is carrying the high surface tensile and compressive loads. The core provides lightweight and structural stability. The combination of sheets of aluminium alloy with laminates of fibre-reinforced resin, as in the commercial product ARALL (Aramid-Reinforced Aluminium, Davis, 1985) is a related variety of layered hybrid. A mixing of fibrous and particulate fillers in a single resin or metal matrix produces another kind of hybrid composite.

In high-technology fields the question of cost may be insignificant by comparison with the advantages of optimizing properties. In aerospace applications, purpose of using hybrids is to utilize the natural toughness of GRP or of Kevlar-fibre-reinforced plastics (KFRP) to avoid brittleness of typical CFRP. The important aspect of using hybrids is to provide adequate material stiffening, strengthening and toughening, composite to suit specific requirements which produce a single-fibre types of composites. The advanced structural fibres, such as E-Glass, S-Glass, Kevlar, Carbon fibres, are taken for simulation study and amplitude of vibration single link robotic manipulator estimated.

2.2. Methodology

The terminology and model arrangement of a flexible manipulator working system as shown in Figure 1 and Figure 2, aims to formulate an equation of motion for numerical investigation. The flexible link is connected to the hub, the hub attached to the actuator shaft and a gear is provided for joint flexibility in the experimental model. The entire arrangement is enclosed by casing. This arrangement is called hermetically sealed joint which is treated as a flexible joint. Flexibility in joints is energy storing device, which helps the system for low energy consumption.

The length of link 'l' in *meter* and 'ρ' is uniform mass density per unit length in *kg/m*. The joint and link is attached at the rotor shaft of the motor. 'E' and 'I' represent young modulus N/m^2 and area moment of inertia m^4 of link respectively. The angular position is $\theta(t)$ and $u(x, t)$ is the transverse component of the flexible displacement of flexible link. 'M_p' is mass of payload with inertia 'I_p' at the end-point of link are physical parameters of system. The motor clamped to the joint is stationary. 'I_h' is the inertia of the hub and 'K_t' stiffness of spring. The input torque '$\tau(t)$' in Nm is applied to the motor. The single link rotates in a horizontal plane. The co-ordinate frames X_o-O-Y_o and X_1-O-Y_1 are attached to the rigid body frame. Due smaller angular rotation $\theta(t)$ of pinned free robotic manipulator, the flexible deflection $u(x, t)$ and total displacement $y(x, t)$ of a links are calculated as,

$$y(x,t) = u(x,t) + x\theta(t) \tag{1}$$

For equation of motion, the energy associated to the systems is calculated. The kinetic (KE) and potential (PE) energies of the system with end payload are included in equation. In the equation of motion, a non conservative work for a given input torque to the system is calculated. Using Hamilton, and lagrangian techniques, by ignoring the rotary inertia and shear deformation effects, the first two modes are used for modeling, after a mathematical manipulation, the link equation become with four boundary conditions and partial differential equation of fourth order is obtained.

$$EI\frac{\partial^4 y(x,t)}{\partial x^4} + \rho\frac{\partial^2 y(x,t)}{\partial t^2} = 0 \tag{2}$$

The flexible deflection $u(x, t)$ is determined and substituted in the equation which yields the equation of motion in terms total deflection of $y(x, t)$.

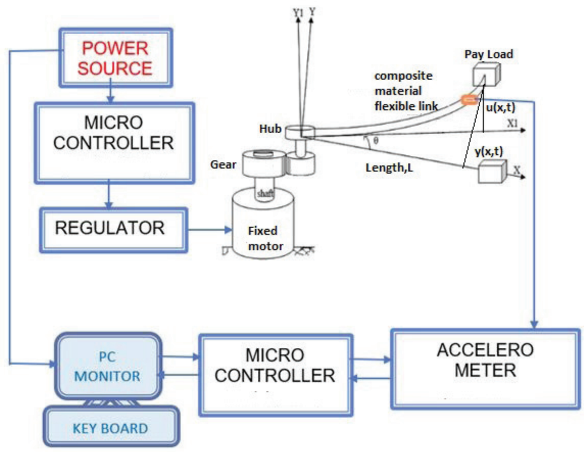

Fig. 1. Block diagram of amplitude measurement setup single link Manipulator

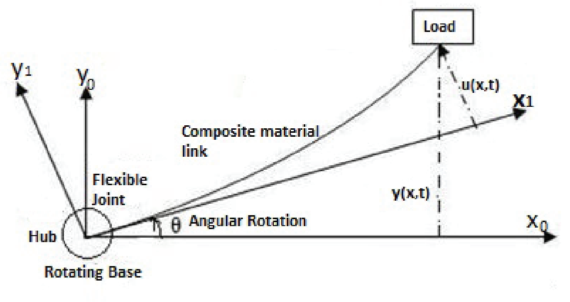

Fig. 2. Schematic diagram of structural fibre single link Manipulator

3. Dynamic Equation

Using the boundary conditions, the obtained fourth order partial differential equation is solved. This equation describes the motion of flexible link manipulator. The solution is obtained by using assumed mode method, and lagrangian approach. The flexible deflection is the product, spatial and time function. The flexible deflection $u(x, t)$ is approximated by,

$$u(x,t)=\sum_{i=1}^{n}\varphi_1(x)q_1(t)+\sum_{i=1}^{n}\varphi_2(x)q_2(t)+\ldots+\sum_{i=1}^{n}\varphi_i(x)q_i(t)$$

$$\text{for } i=1,\ 2,\ 3,\ \ldots,\ n \tag{3}$$

The input torque $(T)_{in}$ is set to zero. The orthogonality relationship of the second derivatives, which is true for a system with only structural flexibility, hence the total flexible deflection from the initial co-ordinate is determined by,

$$y(x,t)=\sum_{i=1}^{n}\varphi_1(x)q_1(t)+\sum_{i=1}^{n}\varphi_2(x)q_2(t)+\ldots+\sum_{i=1}^{n}\varphi_i(x)q_i(t)$$

$$\text{for } i=1,\ 2,\ 3,\ \ldots,\ n \tag{4}$$

The spatial function $\phi_i(x)$ is the mode shape, which is purely function of displacement and $q_i(t)$ time function. To substitute the value of $y(x, t)$ in equation, this yields ordinary differential equation of fourth order and second order equation.

The solution for fourth order equation of motion [11] is,

$$\phi_i(x) \;=\; A_i\sin\beta_i x+B_i\sinh\beta_i x+ \\ +\,C_i\cos\beta_i x+D_i\cosh\beta_i x \tag{5}$$

where, i = 1, 2, 3, ..., n and A_i, B_i, C_i and D_i are mode shape constants. To simplify the computation the following parameters are used for equation,

$$\beta^4=\left(\frac{\rho}{EI}\right)\omega^2,\ \lambda=\beta L$$

$$I_b=\frac{\rho L^3}{3},\ \varepsilon=\frac{I_h}{3I_b} \tag{6}$$

$$\eta=\frac{M_pL^2}{3I_b},\ K_c=\frac{K_t}{EI/L}$$

From the above, the characteristic equations of the system are derived and the equation is solved for its Eigen values,

$$\begin{aligned} D(\lambda) \;&=(-\varepsilon\lambda^4+K_c)[1+\cos\lambda\cosh\lambda+ \\ &+\eta\lambda(\cos\lambda\sinh\lambda-\sin\lambda\cosh\lambda)]- \\ &-\lambda(\sin\lambda\cosh\lambda-\cos\lambda\sinh\lambda+ \\ &+2\eta\lambda\sin\lambda\sinh\lambda)=0 \end{aligned} \tag{7}$$

To find frequencies and mode shapes of the system, the values of λ_i are obtained from the characteristic equation (7) and the corresponding values of constants A_i, B_i, C_i and D_i are also calculated. Assume that the value of D_i =1(one) according to assumed mode method. The normalization relations, the expression for kinetic and potential energy are determined.

Tab. 1. System mode parameters λ_i (i = 0, 1, 2, 3, 4) for rigid and flexible joint with Load

ε	K_c	η	Modes				
			λ_0	λ_1	λ_2	λ_3	λ_4
0.05	0	1	0	2.6303	4.3386	7.1904	10.2753
0.05	1	1	-	0.8657	2.7899	4.3563	7.1909
0.05	5	1	-	1.1009	3.2175	4.4409	7.1927

3.1. System State Space Model

The equation of motion using assumed mode, Hamilton principle [12] with lagrangian technique are used to derive the equation. The equations are in the form of a state space model which utilized for simulation analysis. The equations of the state space form [13] and [14] for two modes.

$$X^{\bullet}=AX+Bu \tag{8}$$

$$\begin{bmatrix} q_o' \\ q_o'' \\ q_1' \\ q_1'' \\ q_2' \\ q_2'' \end{bmatrix}=\begin{bmatrix} 0 & 1 & 0 & 0 & 0 & 0 \\ 0 & 0 & 0 & 0 & 0 & 0 \\ 0 & 0 & 0 & 1 & 0 & 0 \\ 0 & 0 & -\omega_1^2 & -2\xi_1\omega_1 & 0 & 0 \\ 0 & 0 & 0 & 0 & 0 & 1 \\ 0 & 0 & 0 & 0 & -\omega_2^2 & -2\xi_2\omega_2 \end{bmatrix}\begin{bmatrix} q_o \\ \dot{q}_o \\ q_1 \\ \dot{q}_1 \\ q_2 \\ \dot{q}_2 \end{bmatrix}+\frac{1}{I_T}\begin{bmatrix} 0 \\ 1 \\ 0 \\ \frac{d}{dx}\phi_1(0) \\ 0 \\ \frac{d}{dx}\phi_2(0) \end{bmatrix}\tau \tag{9}$$

4. Simulation Analysis

The vibration mode analysis is significant in accurate model of flexible of the system [15]. In this system the development of the single link model and mode analysis are carried out.

The mathematical equation was derived based on Lagrangian and assumed mode method (AMM) with orthogonality condition [16]. Finally transformed into state space model in equation (9) is used for simulation and modes were drawn with corresponding frequency.

4.1. Types of Structural Fibre

The five different variety of structural fibre manipulator have taken to examine the mode amplitude of vibration in terms of end point displacement and end point residual. Flexible composite structural fibre manipulators are made of combination of the material E- Glass, S- Glass epoxy, Kevlar epoxy and Carbon epoxy. The parameters are listed in Table1 for use of simulation.

Tab. 2. Typical properties of structural fibre

SL. No	Type of Fibre	Fibre Density kg/m^3	Young's modulus Gpa	Tensile stress Gpa	Fibre Elongation %
1	E-Glass	2.54	72.5	1.72-3.45	2.5
2	S-Glass	2.49	87	2.53-4.48	2.9
3	Kevlar 29	1.45	85	2.27-3.80	2.8
4	Kevlar 49	1.45	117	2.27-3.80	1.8
5	Carbon HS	1.80	227	2.80-5.10	1.1
6	Carbon HM	1.8-1.86	370	1.80	0.5
7	Carbon UHM	1.86-2.10	350-520	1.00-1.25	0.2

4.2. E-Glass Structural Fibre

The E-Glass structural material for flexible single link manipulator is used to examine the dynamic performance. The amplitude mode of vibration plotted, size of the link and their parameter are given in the Table 2. The geometrical size of the link is constant for all five cases.

Tab. 3. E-Glass Structural fibre parameter

Parameters	Symbol	Units
Length	L	0.25m
Width	b	0.025m
Thickness	d	0.002m
Area	A	$5e^{-5}m^2$
Weight density	ρ_c	$1.2700e^{-04}$ kg/m
Weight of Link	W_L	$3.1750e^{-05}$ kg
Second MOI	I	$1.6667e^{-11}m^4$
Young modulus	E	$72.5e^9 N/m^2$
Rigidity	EI	1.2083 Nm^2
Inertia of beam	I_b	$6.6146e^{-07}$ kg m^2
Hub Inertia	I_h	$9.9219e^{-08}$ kgm^2

4.2.1. E-Glass Mode Plots

The composite structural fibre flexible link robotic manipulator is made of E-Glass with epoxy. Using data, the response of a link is simulated through step input torque for under damped condition. The program is carried for 0.3 seconds for first mode and other modes are 0.1seconds. The output response of advanced composite fibre manipulators link are observed. The mode-1, mode-2, for three types of joint flexibilities are shown in Figures 3 and 4. The amplitude of vibration is reduced when the joint flexibility is high (k_c=5). The steady state at 0.04seconds in second modes.

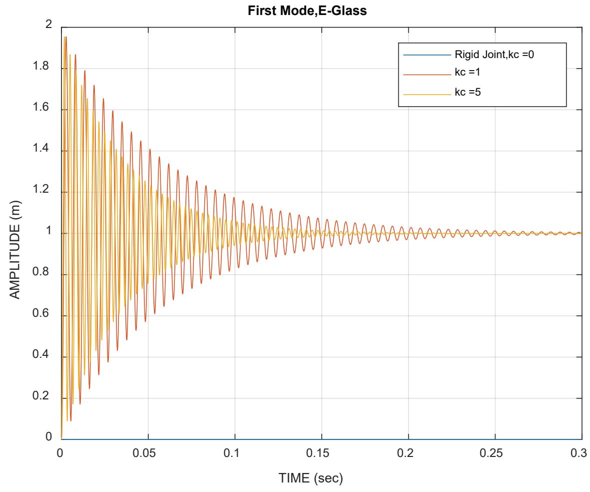

Case 1: k_c = 0, λ_0 = 0, Case 2: k_c =1, λ_1 = 0.8657
Case.3: k_c = 5, λ_1=1.1009.

Fig. 3. First mode-3 types of Joint flexibility

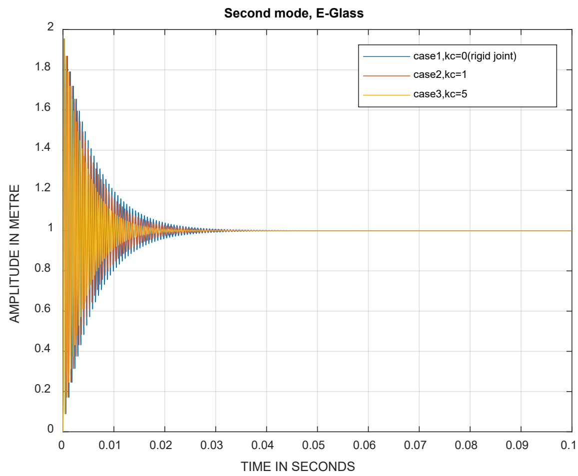

Case 1: k_c =0, λ_1 =2.630312, Case 2: k_c = 1, λ_2=2.7899,
Case.3: k_c = 5, λ_2 = 3.2175

Fig. 4. Second mode-3 types of Joint flexibility

4.3. S-Glass Structural Fibre

The E-Glass properties are modified, resulted S-GLASS fibre with improved properties and compositions are SiO_2–65%, Al_2O_2–25%, MgO-10%. It has plenty of merits such as higher production rate, improved mechanical properties, high strength, high stiffness, relatively low density, non flammable, resistant to heat, good chemical resistance, relatively insensitive to moisture, and able to maintain strength with wide range of condition. Their applications in the areas are military missiles, aircraft structures, laminate structures, storage tanks, composite and surf boards (Table 3).

Tab. 4. S-Glass Structural fibre parameter

Parameters	Symbol	Units
Length	L	0.25m
Width	b	0.025m
Thickness	d	0.002m
Area	A	$5e^{-5}m^2$
Weight density	ρ_c	$1.2450e^{-04}$ kg/m
Weight of Link	W_L	$3.1125e^{-05}$kg
Second MOI	I	$1.6667e^{-11}m^4$
Young modulus	E	$87e^9N/m^2$
Rigidity	EI	$1.4500Nm^2$
Inertia of beam	I_b	$6.4844e^{-07}$ kgm^2
Hub Inertia	I_h	$9.7266e^{-08}$

4.3.1. S-Glass Mode Plots

The S-glass fibre simulations for same size link are carried out. The output responses are noted for mode-1, mode-2, for three types of joint flexibilities in link system (Figures 5 and 6).

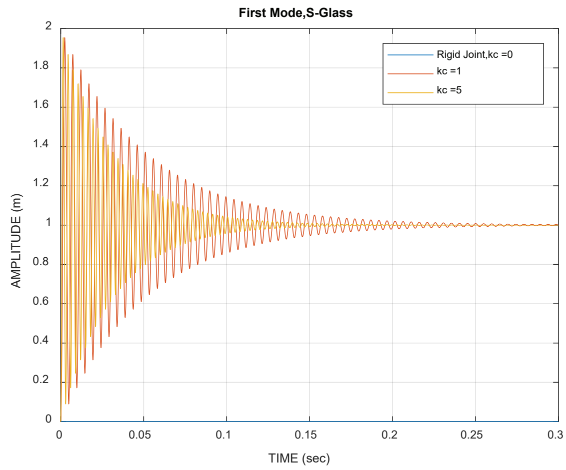

Case 1: $k_c = 0$, $\lambda_0 = 0$, Case 2: $k_c = 1$, $\lambda_1 = 0.8657$
Case.3: $k_c = 5$, $\lambda_1 = 1.1009$.

Fig. 5. First mode-3 types of Joint flexibility

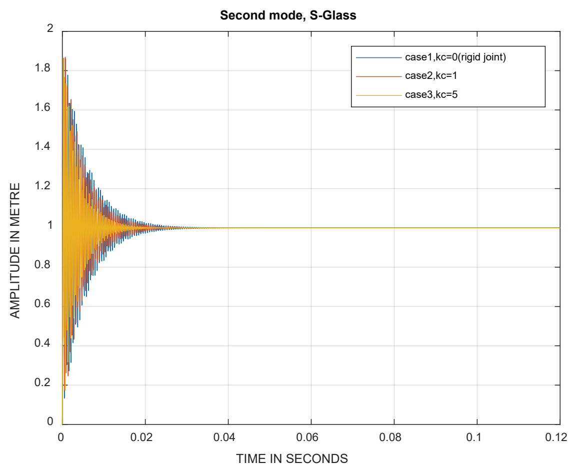

Case 1: $k_c = 0$, $\lambda_1 = 2.630312$, Case 2: $k_c = 1$, $\lambda_2 = 2.7899$,
Case.3: $k_c = 5$, $\lambda_2 = 3.2175$

Fig. 6. Second mode-3 types of Joint flexibility

4.4. Kevlar-29 Structural Fibre

This type of material compared to steel is twenty times stronger. The material types are (1) Kevlar- 29 (2) Kevlar- 49. These materials have wide range of application such as, water proof walking boots, car/motor bike tyre, and armour panels for light weight vehicles, fire resistance clothing, making cables, asbestos, brake linings etc, and making body of vehicles etc. The data for Kevlar-29 given Table 4.

Tab. 5. Kevlar-29 Structural fibre parameter

Parameters	Symbol	Units
Length	L	0.25m
Width	b	0.025m
Thickness	d	0.002m
Area	A	$5e^{-5}m^2$
Weight density	ρ_c	$7.2500e^{-05}$kg/m
Weight of Link	W_L	$1.8125e^{-05}$kg
Second MOI	I	$1.6667e^{-11}m^4$
Young modulus	E	$85e^9N/m^2$
Rigidity	EI	$1.4167Nm^2$
Inertia of beam	I_b	$3.7760e^{-07}$kgm^2
Hub Inertia	I_h	$5.6641e^{-08}$ kgm^2

4.4.1. Kevlar-29 Mode Plots

By using MATLAB coding, the output response of first mode is 0.3 seconds and 0.1seconds for other modes. The output response of advanced composite fibre KEVLAR-29 manipulators link is observed and noted that the steady state time is reduced. The mode-1, mode-2, mode-3 and mode-4 for three types of joint flexibilities are shown in Figures 7and 8. The steady state is at 0.15sec for first mode when $k_c = 5$.

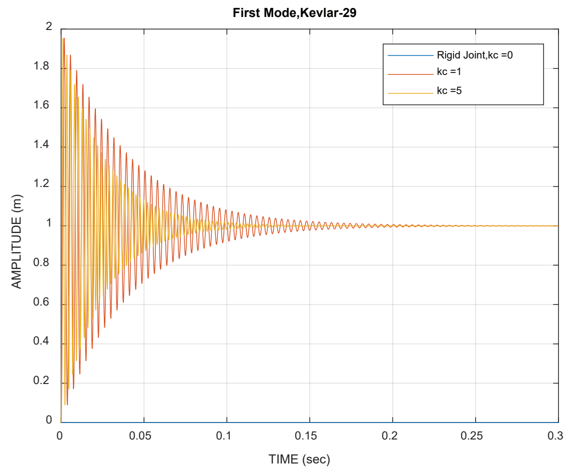

Case 1: $k_c = 0$, $\lambda_0 = 0$, Case 2: $k_c = 1$, $\lambda_1 = 0.8657$
Case.3: $k_c = 5$, $\lambda_1 = 1.1009$.

Fig. 7. First mode-3 types of Joint flexibility

4.5. Kevlar-49 Structural Fibre

The physical properties of Kevlar-49 are given in the Table 5. The application of Kevlar-49 in the areas like, boat hulls, aerospace industry, military planes, good resistance when hit by small arms and high modulus are used in cable and rope products.

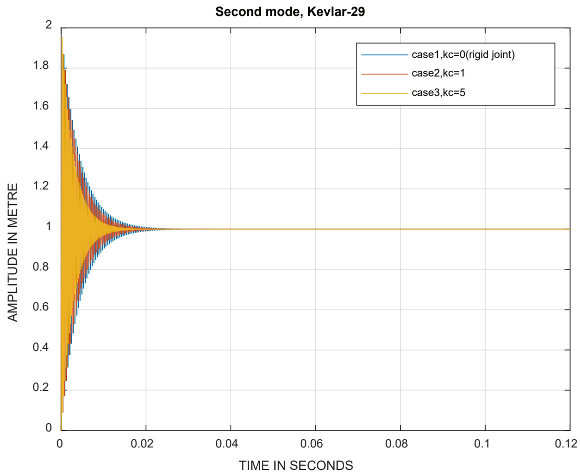

Case 1: k_c=0, λ_1=2.630312, Case 2: k_c= 1, λ_2=2.7899,
Case.3: k_c= 5, λ_2= 3.2175

Fig. 8. Second mode-3 types of Joint flexibility

Tab. 6. Kevlar-49 Structural fibre parameter

Parameters	Symbol	Units
Length	L	0.25m
Width	B	0.025m
Thickness	D	0.002m
Area	A	5e-5m²
Weight density	ρ_c	7.2500e-05kg/m
Weight of Link	W_L	1.8125e-05kg
Second MOI	I	1.6667e-11 m⁴
Young modulus	E	117e⁹N/m²
Rigidity	EI	1.9500Nm²
Inertia of beam	I_b	3.7760e-07kgm²
Hub Inertia	I_h	5.6641e-08 kgm²

4.5.1. Kevlar-49 Mode Plots

The output response of the link using Kevlar-49 and simulation time for first mode is 0.3 seconds and remaining modes are 0.1seconds. The output responses are noted that the steady state time reduced. But the oscillations are increased. The mode-1, mode-2, for three types of joint flexibilities are given in Figures 9 and 10.

4.6. Carbon-HS Structural Fibre

The carbon fibres are produced using various raw materials, provided their chemical compound has high carbon content. In general, polyacrylnitrile (PAN), pitch or rayon/viscose (e.g. biocomposites) is used. PAN is manufactured product with well defined properties. Pitch is a natural product. Threads drawn from PAN or pitch pass through three stages: oxidation at approximately 200°C, carbonization at 800-1600°C and ultimately graphitization. The fibres are stretched during this process, and an anisotropic fibre is formed. Carbon fibres are often transversally isotropic and have a much higher stiffness in the transverse direction [17]. The mechanical properties are improved outstanding way by adding carbon fibres [18].

Tab. 7. Carbon-HS Structural fibre parameter

Parameter	Symbol	Units
Length	L	0.25m
Width	B	0.025m
Thickness	D	0.002m
Area	A	5e-5m²
Weight density	ρ_c	9.0000e-05
Weight of Link	W_L	2.2500e-05
Second MOI	I	1.6667e-11m⁴
Young modulus	E	227e⁹N/m²
Rigidity	EI	3.7833 Nm²
Inertia of beam	I_b	4.6875e-07 kgm²
Hub Inertia	I_h	7.0313e-08 kgm²

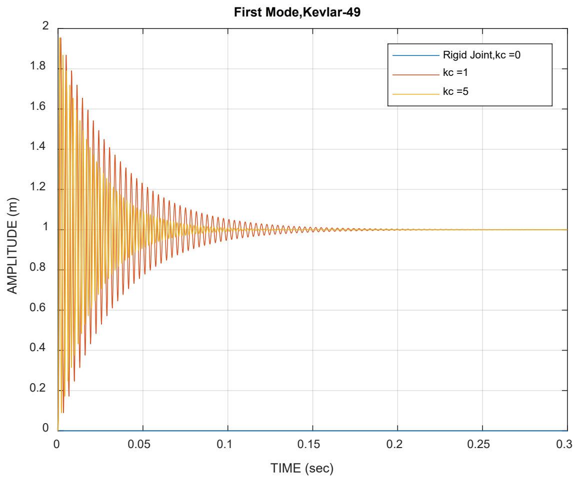

Case 1: k_c = 0, λ_0 = 0, Case 2: k_c =1, λ_1 = 0.8657
Case.3: k_c = 5, λ_1=1.1009.

Fig. 9. First mode-3 types of Joint flexibility

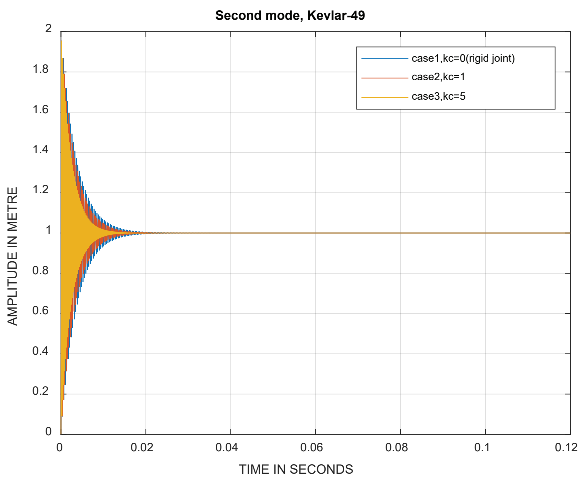

Case 1: k_c =0, λ_1 =2.630312, Case 2: k_c = 1, λ_2=2.7899,
Case.3: k_c = 5, λ_2 = 3.2175

Fig. 10. Second mode-3 types of Joint flexibility

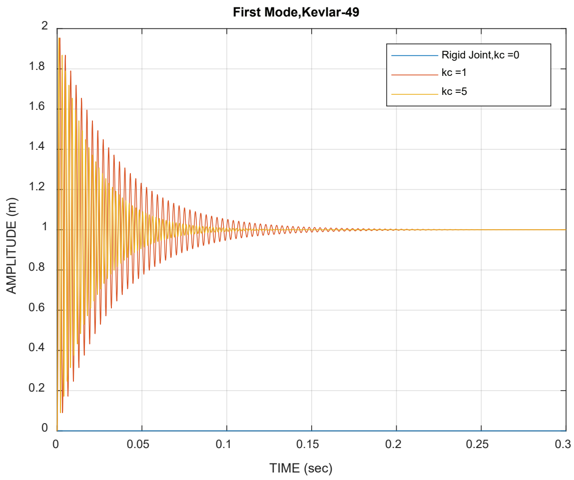

Case 1: $k_c = 0$, $\lambda_0 = 0$, Case 2: $k_c = 1$, $\lambda_1 = 0.8657$
Case.3: $k_c = 5$, $\lambda_1 = 1.1009$.

Fig. 9. First mode-3 types of Joint flexibility

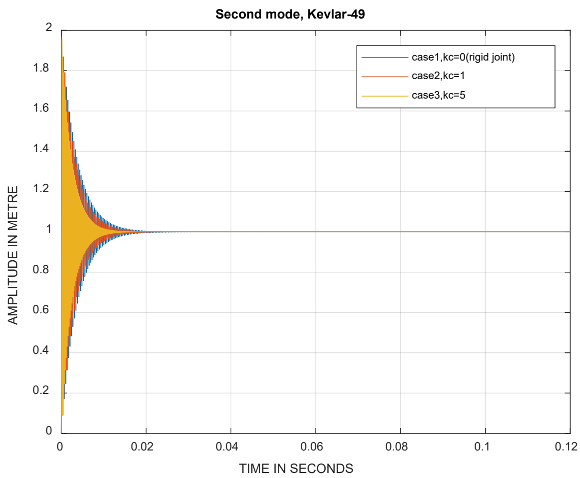

Case 1: $k_c = 0$, $\lambda_1 = 2.630312$, Case 2: $k_c = 1$, $\lambda_2 = 2.7899$,
Case.3: $k_c = 5$, $\lambda_2 = 3.2175$

Fig. 10. Second mode-3 types of Joint flexibility

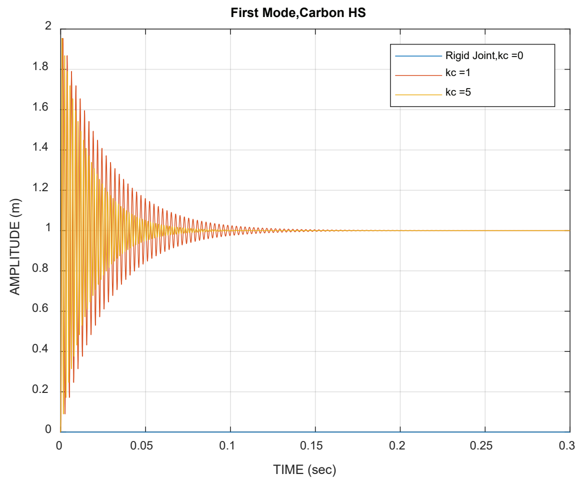

Case 1: $k_c = 0$, $\lambda_0 = 0$, Case 2: $k_c = 1$, $\lambda_1 = 0.8657$
Case 3: $k_c = 5$, $\lambda_1 = 1.1009$.

Fig. 11. First mode-3 types of Joint flexibility

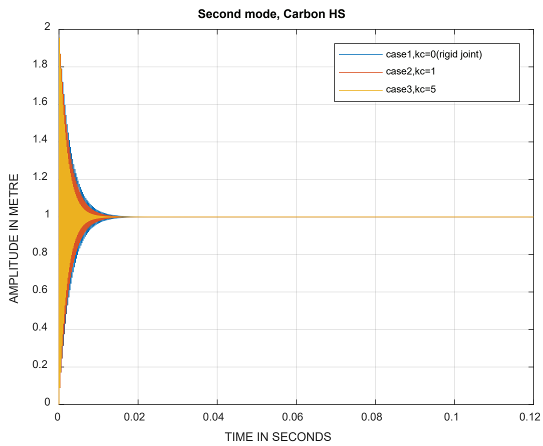

Case 1: $k_c = 0$, $\lambda_1 = 2.630312$, Case 2: $k_c = 1$, $\lambda_2 = 2.7899$,
Case 3: $k_c = 5$, $\lambda_2 = 3.2175$

Fig. 12. Second mode-3 types of Joint flexibility

4.6.1. Carbon-HS Mode Plots

The CARBON-HS mode response plots for single flexible link manipulator are simulated and amplitude modes of vibration, for four modes with different stiffness co-efficient are given in Figures.11 and 12.

5. Results and Discussion

The system mode parameters λ_i based on the characteristic equation of a flexible system was determined and it was noticed that the stiffness co-efficient for flexible system is not equal to zero. This means no zero-mode flexible link system (λ_i not equal to zero). The response of the system using step input torque was calculated and simulation results were shown in Figures 3-12. The link was made of composite structural fibre material such as E-Glass fibre, S-Glass fibre Kevlar-29, Kevlar-49, and carbon HS are taken five different cases for simulation study. The natural frequency and mode were calculated using Eigen value approach. The frequency response function (FRF) of the system was obtained by MATLAB.

The link has a uniform rectangular cross section with size 25mm x 2mm and length was 250mm. The geometric parameters were constant for all five types. The other parameters were found and listed in the Tables 1-7. The problem was analyzed making use of the solution obtained by the method briefed. The natural frequency was calculated. By introducing the viscous damping co-efficient to each mode, and the damped natural frequencies were calculated. The modes to the corresponding natural frequency are plotted as shown Figures 3-12.

5.1. E-Glass

A comparative study with different joint flexibility were made in order to exhibit the importance of the both joint and link flexibility in the model, i.e., case-1 stiffness of the joint $k_c = 0$, case-2 stiffness of the joint $k_c = 1$, case-3 stiffness of the joint $k_c = 5$. The Figure 3 and 4 gives the first, second, modes of E-Glass material flexible link with varying joint stiffness co-efficient. The maximum vibration amplitude for first mode of three types joint flexibility of links i.e., case-1 $k_c = 0$, case-2 $k_c = 1$, case-3 $k_c = 5$. i.e., are 0, 0.151m and 0.122 m. The maximum vibration amplitude for second mode case1, i.e. rigid mode stiffness co-efficient ($k_c = 0$) is 0.213m, case-2 ($k_c = 1$) is 0.212m, case-3 ($k_c = 5$) is 0.200m.

For third mode the maximum vibration amplitude for case1, case-2, and case-3 are 0.00012m, 0.000074m and 0.000024m respectively. The Fourth mode amplitude of vibration are case1 ($k_c = 0$), case-2 ($k_c = 1$), case-3 ($k_c = 5$), are 0.0000256 m, 0.0000254m and 0.0000024m respectively. The values of third and fourth mode compared to the first and second modes are very low. This shows that the amplitudes for higher mode values are very small, and noticed a reduced model which considers first two modes could be used for controller design.

5.2. S-Glass

The Figure 5 and 6 gives the first, second, modes of S-glass material flexible link with varying joint stiffness co-efficient. The maximum vibration amplitude for first mode of three types joint flexibility of links i.e., case-1 $k_c = 0$, case-2 $k_c = 1$, case-3 $k_c =5$. i.e., are 0, 0.189m and 0.185 m. The maximum vibration amplitude for second mode case1, i.e. rigid mode stiffness co-efficient ($k_c = 0$) is 0.185m, case-2 ($k_c =1$) is 0.183m, case-3 ($k_c =5$) is 0.180m.

5.3. Kevlar-29

The Figure 7 and 8 gives the first, second, modes of KEVLAR-29 material flexible link with varying joint stiffness co-efficient. The maximum vibration amplitude for first mode of three types joint flexibility of links i.e., case-1 $k_c = 0$, case-2 $k_c = 1$, case-3 $k_c =5$. i.e, are 0, 0.188 m and 0.187 m. The maximum vibration amplitude for second mode case-1, i.e. rigid mode stiffness co-efficient ($k_c = 0$) is 0.200 m, case-2 ($k_c = 1$) is 0.189 m, case-3 ($k_c = 5$) is 0.188 m.

5.4. Kevlar-49

The Figure 9 and 10 gives the first, second, modes of KEVLAR-49 material flexible link with varying joint stiffness co-efficient. The maximum vibration amplitude for first mode of three types joint flexibility of links i.e., case-1 $k_c = 0$, case-2 $k_c = 1$, case-3 $k_c =5$. i.e. are 0, 0.189m and 0.188 m. The maximum vibration amplitude for second mode case1, i.e. rigid mode stiffness co-efficient ($k_c = 0$) is 0.200m, case-2 ($k_c =1$) is 0.199m, case-3 ($k_c =5$) is 0.191m.

5.5. Carbon-HS

The Figure 11 and 12 gives the first, second, modes of CARBON-HS material flexible link with varying joint stiffness co-efficient. The maximum vibration amplitude for first mode of three types joint flexibility of links i.e., case-1 $k_c = 0$, case-2 $k_c = 1$, case-3 $k_c =5$. i.e. are 0, 0.200m and 0.200 m. The maximum vibration amplitude for second mode case1, i.e. rigid mode stiffness co-efficient ($k_c = 0$) is 0.200m, case-2 ($k_c =1$) is 0.199m, case-3 ($k_c =5$) is 0.191m.The inclusion of joint flexibility cuts down the amplitudes and total deflection, but increases the oscillatory behavior of the flexible link in the initial stage itself. If the joint flexibilities are excluded, large error would be the result. As a result, a controller design based on the rigid joint would probably be ineffective and possible with flexible joint.

6. Conclusion

In structural fibre flexible link manipulator system, from characteristic equation the Eigen values (λ_i) were found. The corresponding natural frequencies, damped natural frequencies and modes are evaluated. The values of third and fourth modes were compared with simulation plots which shown very low values. But the system initial stages itself increases the oscillatory behavior motion of the composite fibre material link. Further it was noticed that the amplitude of higher modes are numerically low values, therefore the first two modes are used for controller design. The steady state for composite materials for the first and second modes are 0.3sec, 0.03sec. for E-Glass, 0.25sec, 0.025sec for S-Glass. 0.25sec, 0.02sec for KEVLAR-29. 0.158sec, 0.019sec for KEVLAR-49 and 0.1sec, 0.001sec carbon HS. The steady state is very fast in carbon fibre but increased oscillatory behavior. The inclusion of joint flexibility was reduced the total deflection all materials, but increased the oscillatory behavior initially itself. If the joint flexibilities are excluded, large error would be the result. As a result, a controller design based on the flexible joint would be successful compared to rigid manipulator. The controller design is under progress for the above cases.

AUTHORS

S Ramalingam* – Department of Mechanical Engineering, B S Abdur Rahman Crescent Institute of Science and Technology, Chennai, India, email: sengalaniramalingam@gmail.com, suram_ar@rediffmail.com.

S Rasool Mohideen – School of Mechanical Science, B S Abdur Rahman Crescent Institute of Science and Technology, Chennai, India, email: dean.sms@crescent.education.

*Corresponding author

REFERENCES

[1] Q. Liu, Y. Lin, Z. Zong, G. Sun, Q. Li, "Lightweight design of carbon twill weave fabric composite body structure for electric vehicle", *Composite Structures*, vol. 97, 2013, 231–238 DOI: 10.1016/j.compstruct.2012.09.052.

[2] G. Sucharitha, S. Ramalingam, "Optimization and Improvement of Material Handling System", *International Journal of Pure and Applied Mathematics,* Special Issue, vol. 116, no. 17, 2017, 185–190.

[3] E. Şahin, "Swarm Robotics: From Sources of Inspiration to Domains of Application". In: *Swarm Robotics*, 2005, 10–20 DOI: 10.1007/978-3-540-30552-1_2.

[4] S. Ramalingam, S. R. Mohideen, S. Manigandan, T. P. P. Anand, "Hybrid polymer composite material for robotic manipulator subject to single link flexibility", *International Journal of Ambient Energy*, 2018, 1–8 DOI: 10.1080/01430750.2018.1557551.

[5] S. Ramalingam, S. R. Mohideen, "Composite materials for advanced flexible link robotic manipulators: an investigation", *International Journal of Ambient Energy*, 2019, 1–6 DOI: 10.1080/01430750.2019.1613263.

[6] K. Shimoga, A. Goldenberg, "Soft materials for robotic fingers". In: *Proceedings of 1992 IEEE International Conference on Robotics and Automation*, 1992, 1300–1305 DOI: 10.1109/ROBOT.1992.220069.

[7] A. Albu-Schaffer, O. Eiberger, M. Grebenstein, S. Haddadin, C. Ott, T. Wimbock, S. Wolf, G. Hirzinger, "Soft robotics", *IEEE Robotics Automation Magazine*, vol. 15, no. 3, 2008, 20–30 DOI: 10.1109/MRA.2008.927979.

[8] B. A. Trimmer, A. E. Takesian, B. Sweet, C. Rogers, D. Hake, D. J. Rogers, "Caterpillar locomotion: A new model for soft-bodied climbing and burrowing robots". In: *7th International Symposium on Technology and the Mine Problem,* Monterey, CA May 2-5, 2006.

[9] H. Lipson, "Challenges and Opportunities for Design, Simulation, and Fabrication of Soft Robots", *Soft Robotics*, vol. 1, no. 1, 2014, 21–27 DOI: 10.1089/soro.2013.0007.

[10] S. I Wayan, S. I Gusti Agung Kade, K. Arnis, "Mechanical Properties of Rice Husks Fiber Reinforced Polyester Composites", *International Journal of Materials, Mechanics and Manufacturing*, vol. 2, no. 2, 2014, 165–168 DOI: 10.7763/IJMMM.2014.V2.121.

[11] W. T. Thomson, *Theory of vibration with applications*, 3rd ed., Prentice-Hall, 1988.

[12] R. R. Craig, *Structural dynamics: an introduction to computer methods*, Wiley, 1981.

[13] M. O. Tokhi, A. K. Azad, *Flexible Robot Manipulators: Modelling, simulation and control*, IET Digital Library, 2008.

[14] K. Ogata, *Modern control engineering*, Pearson Education, 2010.

[15] K. Ibrahim, A. A. Aly, A. A. Ismail, "Mode Shape Analysis of a Flexible Robot Arm", *International Journal of Control, Automation and Systems*, vol. 2, no. 1, 2013.

[16] S. Ramalingam, S. Rasool Mohideen, "Numerical Analysis of Robotic Manipulator Subject to Mechanical Flexibility by Lagrangian Method", *Proceedings of the National Academy of Sciences, India Section A: Physical Sciences*, 2019 DOI: 10.1007/s40010-019-00619-2.

[17] J. Obradovic, S. Boria, G. Belingardi, "Lightweight design and crash analysis of composite frontal impact energy absorbing structures", *Composite Structures*, vol. 94, no. 2, 2012, 423–430 DOI: 10.1016/j.compstruct.2011.08.005.

[18] A. Mohajerani, S. Hui, M. Mirzababaei, A. Arulrajah, S. Horpibulsuk, A. Abdul Kadir, M. T. Rahman, F. Maghool, "Amazing Types, Properties, and Applications of Fibres in Construction Materials", *Materials*, vol. 12, no. 16, 2019 DOI: 10.3390/ma12162513.